JOURNAL OF IRON AND STEEL RESEARCH, INTERNATIONAL. 2010, 17(3): 34-39

Influence of Specimen Geometry of Hot Torsion Test on Temperature Distribution During Reheating Treatment of API-X70

Bahman Mirzakhani[1], Shahin Khoddam[2], Hossein Arabi[3], Mohammad Taghi Salehi[3], Seyed Hossein Seyedein[3], Mohammad Reza Aboutalebi[3]

(1. Faculty of Engineering, Arak University, Arak 38156-879, Iran; 2. Department of Mechanical Engineering, Monash University, Clayton Campus, Vic 3800, Australia; 3. Department of Materials and Metallurgical Engineering, Iran University of Science and Technology, Tehran 16844-13114, Iran)

Abstract: The commercial finite element package ANSYS™ was utilized for prediction of temperature distribution during reheating treatment of hot torsion test (HTT) samples with different geometries for API-X70 microalloyed steel. Simulation results show that an inappropriate choice of test specimen geometry and reheating conditions before deformation could lead to non-uniform temperature distribution within the gauge section of specimen. Therefore, assumptions of isothermal experimental conditions and zero temperature gradient within the specimen cross section appear unjustified and led to uncertainties of flow curve obtained. Recommendations on finding proper specimen geometry for reducing temperature gradient along the gauge part of specimen will be given to create homogeneous initial microstructure as much as possible before deformation in order to avoid uncertainty in consequent results of HTT.

Key words: hot torsion test; simulation; specimen geometry; reheating treatment; microalloyed steel

The hot torsion test (HTT) has been one of the most popular mechanical tests for assessment of workability of metals and alloys for bulk forming processes during last decades[1-6]. It is often chosen over the uniaxial tension and compression tests because very large strain and strain rates can be achieved without the problems of necking and barreling, respectively[7]. In this test the effective strain and effective stain rate are as function of gauge length and radius. So to overcome the test rig limitations a wide range of specimen geometries and sizes have been used in different studies[1-6] in order to obtain the required strain and strain rate range.

The reheating treatment is the first stage of thermomechanical processes in order to obtain homogeneous composition before doing hot rolling or hot forging. The effect of pre-deformation reheating treatment on microstructure evolution such as initial austenite grain size and behavior of microalloying elements has been investigated in several studies[6,8-12]. These investigations deduce that austenitizing temperature has a great influence on initial microstructure and consequence deformation behavior of steels.

In simulation of thermomechanical process via HTT, before starting the hot torsion testing, the material is usually heated to the given temperature as a reheating temperature and soaked for a while and then cooled to the deformation temperature. In hot torsion machines the heating energy usually is supplied by an induction or resistance type furnace[1-3,13-15]. The influences of specimen geometry of HTT and reheating conditions have not been investigated systematically. However, no proper consideration of these choices may introduce some errors in consequence results of test due to the non-uniform initial temperature and microstructure within the material.

At the present study, the commercial finite element package ANSYS™ was used to investigate the effects of specimen geometry and process conditions on distribution of temperature within the specimen during reheating treatment. This approach will enable to prevent the high temperature gradient within

Biography: Bahman Mirzakhani(1977—), Male, Doctor; **E-mail**: b-mirzakhani@araku.ac.ir; **Received Date**: August 15, 2008

specimen by finding optimum geometry and reheating conditions to obtain homogenous initial microstructure before starting HTT.

It is worth noting that the present model developed on the base of a flexible hot torsion test machine, has been developed at IROST[15].

1 Model and Simulation Conditions

In this study for prediction of temperature distribution during reheating treatment and before hot torsion testing, the commercial FEM code ANSYS™ was used. So according to reheating treatments which almost is used in experiments, a reheating cycle was designed as shown in Fig. 1. The temperatures 740 and 880 ℃ in this figure are A_{c1} and A_{c3} temperatures of present microalloyed steel respectively which were determined by dilatometry test as presented in Fig. 2. In this range rather low heating rate considered in order to give time for ferrite and perlite transformation to austenite. The chemical composition of the API-X70 microalloyed steel used in this study is given in Table 1.

The geometry of the HTT specimen used in this investigation is shown in Fig. 3. A two dimensional FE analysis of heat flow has been used here to study the effect of initial reheating cycle before deformation starts. The specimen dimensions are shown parametrically in order to consider the effect of each dimension. The domain, boundaries and the mesh which were used in ANSYS™ is also presented in

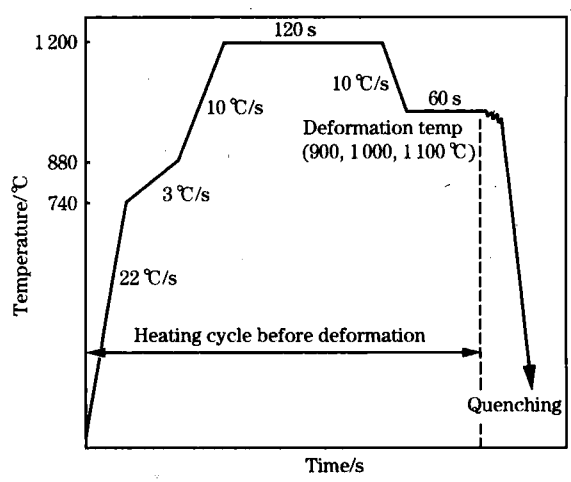

Fig. 1 Reheating cycle before hot torsion test

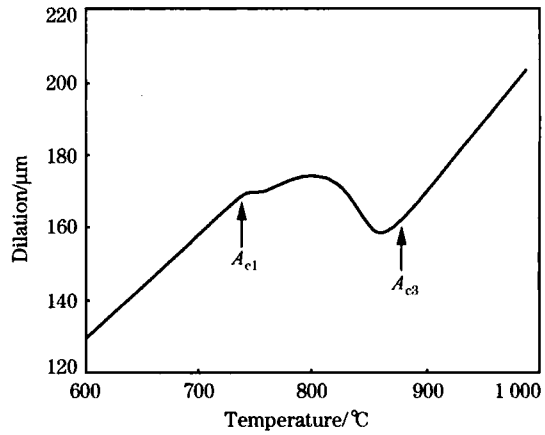

Fig. 2 Dilatation as a function of temperature in dilatometry test

Table 1 Chemical composition of the steel %

C	Mn	Si	P	S	Nb	V	Ti	N	Fe
0.09	1.63	0.32	0.009	0.003	0.04	0.05	0.01	0.002	Rem

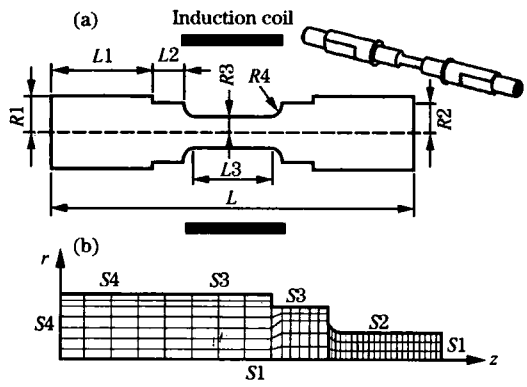

Fig. 3 Schematic of geometry of a solid hot torsion specimen (a) and domain and boundaries and mesh of ANSYS modeling for reheating treatment (b)

Fig. 3 (b) where only one-quarter of a longitudinal section of Fig. 3 (a) is considered because of the symmetry of geometry and the condition with respect to r and z axis.

The axisymmetric conditions during reheating treatment between the body and its environment imply that heat flux along the boundaries S1 is zero or insulated. The boundary S2 is directly heated by an induction coil of 45 mm length. The heating was controlled by a pyrometer carefully located above the center of the specimen. The boundary S3 is exposed to the surrounding environment where the energy loss is considered through both boundary convection and radiation. A simplified approach for radiation

heat transfer was utilized by using an equivalent convection boundary condition in which the non-linearity is considered through a temperature-dependent convection coefficient which will be designated here as h_r:

$$h_r=\tilde{\sigma}\varepsilon[(T_s^2+T_{se}^2)(T_s+T_{se})]_{n-1} \quad (1)$$

where, h_r is equivalent convection coefficient between the body surface S and the surface of the environment enclosing the body at the nth time step; T_s and T_{se} are the absolute temperatures in degrees Kelvin between these surfaces; $\tilde{\sigma}$ is Steffan-Boltzman coefficient; ε is emissivity factor of the surface. The value of $\varepsilon=0.65$ was determined according to the ASTM standard test[16].

The boundary S4 is in contact with grippers of the HTT machine. For these boundaries, the thermal contact conductance (k_{int}) of the interface between the specimen and the grips was considered and heat exchange modeled by convection.

The heat transfer characteristics of the steel of the present work were assumed to be[17-18]: $\rho=7\,800$ kg/m^3, $c=680$ J/(kg · K), $k=36.8$ W/(m · K), $k_{int}=3\,740$ W/(m^2 · K), $T_g=483$ K, $T_a=368$ K, $\tilde{\sigma}=5.67\times10^{-8}$ W/(m^2 · K^4), $h=4$ W/(m^2 · K).

ρ and c are the density and heat capacity of material respectively. Heat convection and heat conduction coefficients are denoted by h and k respectively. The subscripts a, g refer to ambient and grip respectively.

The HTT specimens with different gauge length and radius were designed in order to investigate the effect of specimen geometry on distribution of thermo-mechanical parameters under various deformation conditions. It should be noted that the relationship between the sizes of the specimen, as shown in Fig. 3 (a), were designed according to the basic stiffness requirement expressed in[19-20]. Table 2 summarizes the dimensions of different specimens used in this study.

Table 2 Dimensional description of various HTT specimens mm

Specimen	L1	R1	L2	R2	L3	R3	R4	L
G1	62.0	8	25.0	6.5	8	3.35	1.0	184
G2	62.0	8	12.5	5.5	33	3.35	1.5	184
G3	62.0	8	7.0	6.5	42	3.35	1.5	183
G4	62.0	8	3.0	6.5	52	3.35	1.5	185
G5	57.0	6.25	12.5	4.75	42	2.50	1.5	184
G6	66.5	9.25	3.0	8.0	41	4.25	2.0	184

2 Results and Discussion

Fig. 4 shows the contour plots of temperature distribution in various geometries of HTT specimens after applying reheating cycle (Fig. 1) and before starting deformation at 1 000 ℃.

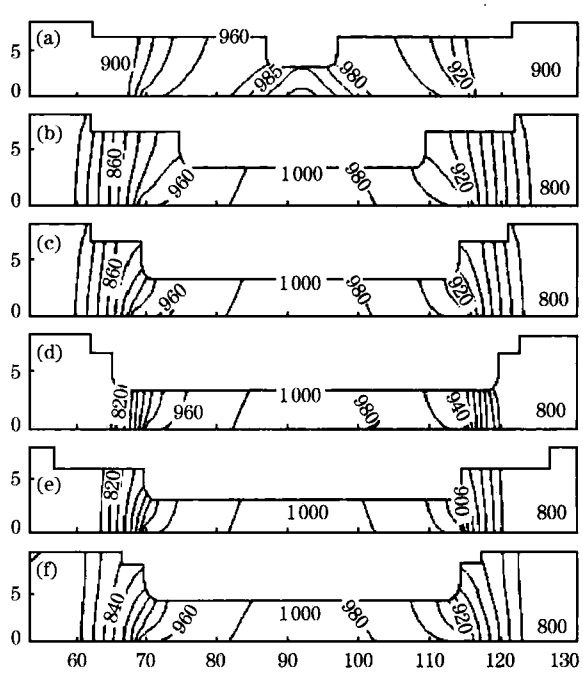

(a) G1; (b) G2; (c) G3; (d) G4; (e) G5; (f) G6.

Fig. 4 Initial temperature distribution in G1, G2, G3, G4, G5, and G6 after applying reheating cycle

This figure illustrates that inductive heating may produce non uniform temperature along the axis of the specimens and caused temperature gradient within gauge part of the sample. In that, in specimens having longer gauge, show greater thermal gradient. For example in G4 (52 mm gauge length) the temperature differential between center and end of the gauge is the largest and about 160 ℃. It should be noted that for all specimens the induction length assumed to be constant and was equal to 45 mm. Sections of specimens located outside of induction coil absorbed the heat of the inside sections and led to lower temperature of ends than center of gauge. This result indicates assumption of uniform temperature distribution in the gauge part of the specimen mentioned in previous works[13-14,17,19] may not be valid. This would have a negative impact on the final results of the test.

The temperature history of two points in the gauge section of G3 during reheating treatment is presented in Fig. 5. It shows that the desirable reheating cycle was only obtained at the center of specimen. The ends of gauge section not only did not reach to appropriate temperature for starting deform-

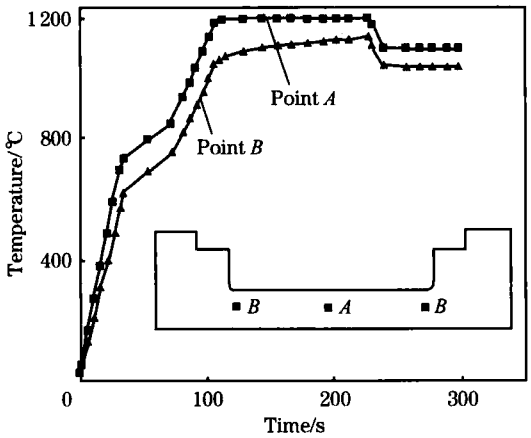

Fig. 5 Time history of two points in gauge section of G3 during reheating treatment

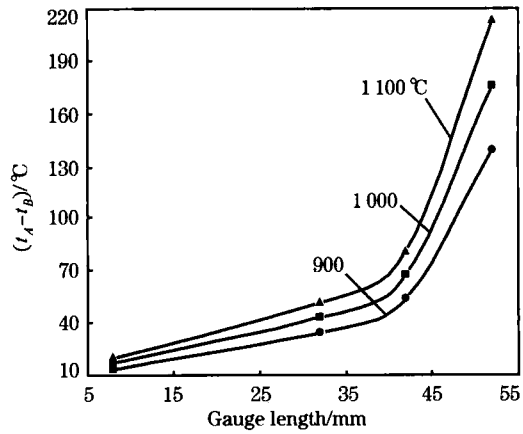

Fig. 6 Effect of gauge length on maximum differential temperature along gauge section

ation but also the desired reheating temperature, i. e. 1 200 ℃, at these points did not achieved. So, it is expected that the solution of the chemical elements will not be occurred completely at these areas. This would fail achievement of a homogeneous composition within specimen before deformation. In addition, different austenitizing temperature at different points of the specimen leads to various initial grain sizes of austenite which is a critical factor that influences subsequent deformation behavior and phase transformation of steel[8-12].

For evaluation of the effect of gauge length on maximum differential temperature along the gauge section and obtain optimum sample geometries, the value of temperature difference between points A and B (t_A-t_B) along the gauge section (Fig. 5) was calculated for various specimens at different temperatures and plotted in Fig. 6. This figure indicates as the gauge length increased; the value of (t_A-t_B) increased; so that for specimen with 52 mm gauge length this gradient exceeded 200 ℃ at 1 100 ℃. It can be also observed that the temperature gradients prior to start of deformation at different temperature are not similar. On the other hand, as temperature of final step decreased the gradient decreased. It relates to the temperature difference between gauge section and other part of the specimen which is less at lower temperatures than higher temperatures. For specimen with short gauge length the temperature did not show much influence on temperature gradient along the sample.

Fig. 7 shows the radial variation of temperature at the center and the end of gauge section after reheating and before the start of deformation at 900, 1 000 and

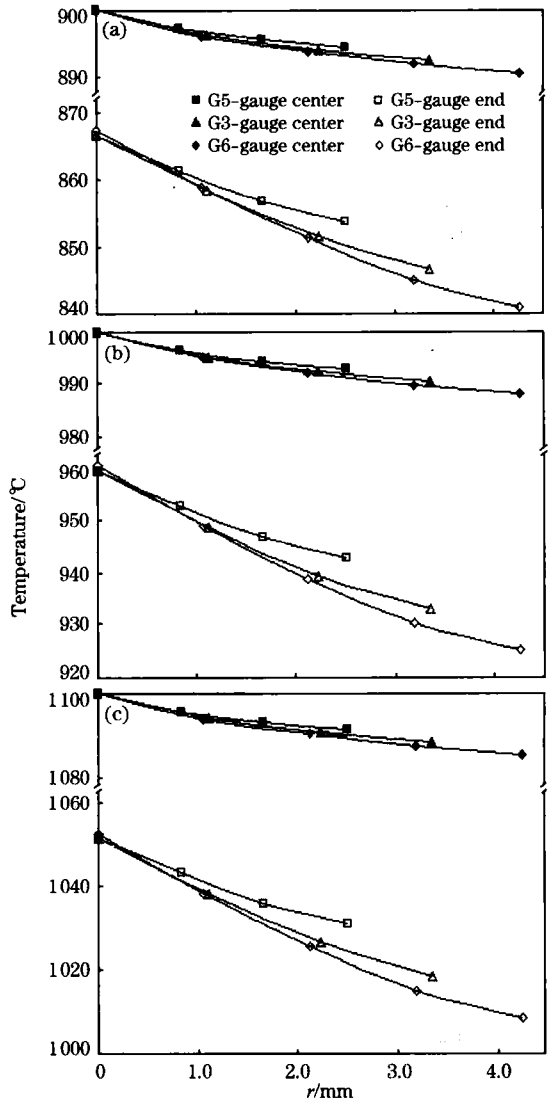

(a) 900 ℃; (b) 1 000 ℃; (c) 1 100 ℃.

Fig. 7 Radial variation of temperature at center and end of gauge section after reheating and before deformation

1 100 ℃. As seen in this figure, temperature decreased along the specimen radius because of heat transfer via convection and radiation from surface of specimen to the surrounding medium. But radial variation of temperature was much less at the center than at the ends of gauge section. It is due to the ends of gauge section are not only adjacent to the end of induction coil but also they are connected to the mini-shoulders and shoulders which absorb a considerable amount of heat generated in the gauge section.

It is worth noting that when the gauge radius increased the slop of temperature vs r curves increased, however this matter is more obvious at the ends than the center of gauge. On the other hand, increasing in gauge radius led to the rate of heating loss along this direction increase. Because according to Table 2, specimens with large gauge diameter have larger mini-shoulder and shoulder diameter in order to stiffness requirement is carried out.

From Fig. 7, influence of finishing temperature of reheating cycle (Fig. 1) on maximum redial gradient in various HTT specimen after reheating was plotted in Fig. 8. When reheating treatment finished at 1 100 ℃ the maximum redial gradient at both center and ends of gauge was greater in comparison of 1 000 ℃ and 900 ℃. However at the center of specimen, temperature difference between surface and core of gauge were less than 45 ℃ and 15 ℃ respectively.

For a given reheating cycle, geometry of HTT specimen have a great influence on temperature distribution after reheating treatment and before deformation

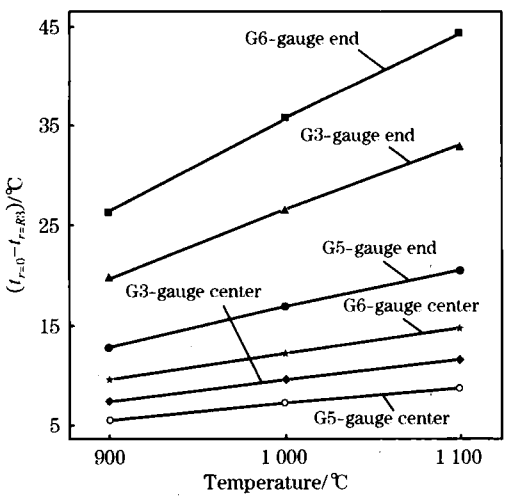

Fig. 8 Influence of finishing temperature of reheating cycle on redial gradient at center and end of gauge section in HTT specimens

as shown in Fig. 6, Fig. 7 and Fig. 8. Various geometries experienced different temperature distribution. In Fig. 9 the result of high gradient temperature with in gauge section of HTT sample on deformation behavior of G4 is illustrated. This sample deformed at 1 100 ℃ and $\omega=10$ rad/s after applying the reheating cycle of Fig. 1. As see in this figure interaction of sever temperature gradient and deformation conditions led to flow localization at the center of specimens. It is due to the mid gauge section experiencing softening phenomena i. e. dynamic recrystallization during deformation; while the ends of the gauge section can not flow as easily as the center.

Fig. 9 Flow localization in G4 specimen deformed at 1 100 ℃ and $\omega=10$ rad/s after applying reheating cycle

Result shows that no proper geometry and dimension selection result in non uniform temperature within specimen and predicted to have effects on the consequence assessment of material behavior during hot deformation as seen in Fig. 9. In addition, it seems prevention of any temperature gradient during reheating treatment of HTT is un-avoidable, but choosing an optimum geometry will minimize this problem. Between different geometries, the specimens G1 and G2 showed the low temperature gradient in both axis and redial directions of the gauge section. Therefore it can be concluded that the optimum geometry are the samples having between 0. 2 and 0. 7 length of induction coil.

3 Conclusion

A numerical modelling was performed to analysis interaction of geometry of hot torsion test specimens and reheating treatment pre-deformation of API-X70 microalloyed steel by the commercial finite element package ANSYS™. Results showed that the specimens in the range of 0. 2 to 0. 7 length of induction coil experienced low temperature gradient in both axial and redial directions after reheating treatment. It seems that these geometries are more reliable for driving accurate constitutive parameters of

the steel by hot torsion test.

The first author is grateful to Arak University for granting a scholarship to him. The authors also acknowledge Sadid Industrial Group for providing the steel.

References:

[1] Samuel F H. Modeling of Flow Stress and Rolling Load of a Hot Strip Mill by Torsion Testing [J]. ISIJ International, 1989, 29(10): 878.

[2] Bia D Q. Effect of Deformation Parameters on the Non-Recrystallization Temperature in Nb-Bearing Steels [J]. Metallurgical Transactions A, 1993, 24: 2151.

[3] Carsi M. The Strain Rate as a Factor Influencing the Hot Forming Simulation of Medium Carbon Microalloyed Steels [J]. Materials Science and Engineering A, 1996, 216: 155.

[4] Hodgson P D. The Prediction of the Hot Strength in Steels With an Integrated Phenomenological and Artificial Neural Network Model [J]. Journal of Materials Processing Technology, 1999, 87: 131.

[5] Quispe A. Improved Model for Static Recrystallization Kinetics of Hot Deformed Austenite in Low Alloy and Nb/V Microalloyed Steels [J]. ISIJ International, 2001, 41(7): 774.

[6] Kuc D. Influence of Deformation Parameters and Initial Grain Size on the Microstructure of Austenitic Steels After Hot-Working Processes [J]. Materials Characterization, 2006, 56: 318.

[7] Dieter G. Handbook of Workability and Process Design [M]. New York: Materials Park, 2003.

[8] Tanaka T. Formation Mechanism of Mixed Austenite Grain Structure Accompanying Controlled-Rolling of Niobium-Bearing Steel [C] // Proceedings of International Conference on Thermomechanical of Microalloyed Austenite. New York: Marcel Dekker, 1981: 195.

[9] Yoshie A. Modelling of Microstructural of Steel Plates Produced by Evolution and Mechanical Properties Thermo-Mechanical Control Process [J]. ISIJ International, 1992, 32(3): 395.

[10] Flores O. Abnormal Grain Growth of Austenite in a V-Nb Microalloyed Steel [J]. Journal of Materials Science, 1997, 32: 5985.

[11] Fernandez A. Static Recrystallization Mechanisms in a Coarse-Grained Nb-Microalloyed Austenite [J]. Metallurgical and Materials Transactions A, 2002, 33: 3089.

[12] Oudin A. Grain Size Effect on the Warm Deformation Behavior of a Ti-IF Steel [J]. Materials Science and Engineering A, 2004, 367: 282.

[13] Zhou M. Thermal Analysis of the Torsion Test Under Hot-Working Condition [J]. Computational Materials Science, 1998, (9): 411.

[14] Njiwa R K. Effect of Self Heating on the Torque vs Equivalent Tensile Strain Plot in High Temperature Torsion of Visco-Plastic Material [J]. Journal of Materials Science, 2001, 36: 5659.

[15] Khoddam S. Conversion of the Hot Torsion Test Results Into Flow Curve With Multiple Regimes of Hardening [J]. Journal of Materials Processing Technology, 2004, 153: 839.

[16] Speidel M. User Guide of OS550/OS550-BB Series Industrial Infrared Thermometer/Transmitter [M]. New York: Marcel Dekker, 1990.

[17] Khoddam S. Thermo-Mechanical Rigid Viscoplastic FE Analysis of the Hot Torsion Test for Determining Constitutive Parameters [D]. Canberra: Monash University, 1997.

[18] Holman J P. Heat Transfer [M]. Boston: McGraw-Hill, 2002.

[19] Khoddam S. The Effect of Specimen Geometry on the Accuracy of the Constitutive Equation Derived From the Hot Torsion Test [J]. Steel Research, 1995, 66(2): 45.

[20] Shigley J E. Mechanical Engineering Design [M]. Boston: McGraw-Hill, 1983.